A quasi-vector finite difference mode solver for optical waveguides with step-index profiles

Jinbiao Xiao (肖金标), Mingde Zhang (张明德), and Xiaohan Sun (孙小菡)

Lab of Photonics and Optical Communications, Department of Electronic Engineering, Southeast University, Nanjing 210096

Received May 8, 2005

A finite difference scheme based on the polynomial interpolation is constructed to solve the quasi-vector equations for optical waveguides with step-index profiles. The discontinuities of the normal components of the electric field across abrupt dielectric interfaces are taken into account. The numerical results include the polarization effects, but the memory requirement is the same as in solving the scalar wave equation. Moreover, the proposed finite difference scheme can be applied to both uniform and non-uniform mesh grids. The modal propagation constants and field distributions for a buried rectangular waveguide and a rib waveguide are presented. Solutions are compared favorably with those obtained by the numerical approaches published earlier.

OCIS codes: 130.2790, 230.7370, 130.0130, 000.4430.

Mode solver for optical waveguides is a key issue in photonic device design. Only a few simple waveguide geometries, however, can be solved analytically, e.g., the one-dimensional slab waveguide or the circular core optical fiber. Therefore, the use of numerical (or approximate) analysis becomes necessary. To perform this task with accuracy, various kinds of numerical techniques[1,2], such as finite difference method (FDM)[3], finite element method (FEM)[4], and mapped Galerkin method (MGM)[5,6], have been proposed. Among them, FDM is an attractive candidate because of the simplicity of its implementation and the sparsity of its resulted matrix.

To date, FDM has been employed to solve both scalar[7] and vector[8] wave equations for optical waveguides with step-index[7,8] even arbitrary-index[3] profiles. In the former case, it is valid only for optical waveguides with very small refractive index difference (say, weakly-guiding waveguides). In the latter case, the optical waveguides with large refractive index difference in regions of high field intensity can be analyzed, but there is a large increase in computational time and memory[1,2]. Instead, the mode solver based on quasi-vector wave equation is a good candidate for optical waveguides, in which the polarization effects of the guided modes are considered, while the memory requirement is the same as that in solving the scalar wave equation. As a result, the computational time is moderate. In addition, Taylor series expansion (TSE) is often used to approximate the resulted quasi-vector wave equation[1,2]. However, the TSE is not easily adaptable to non-uniform grid sizes and extended to account for the discontinuities of the normal components of the electric field across abrupt dielectric interfaces.

In this letter, a modified finite difference scheme is constructed for quasi-vector analysis of optical waveguides with step-index profiles. The polynomial interpolation is employed to convert the quasi-vector wave equation into the finite difference equation in which the discontinuities above-mentioned are taken into account. Moreover, three adjacent grid points are used to approximate each differential operator, so the solution is more accurate than that uses two adjacent grid points. In addition, the present scheme can be applied to both uniform and non-uniform mesh grids.

The quasi-vector wave equation based on electric fields derived from the Maxwell's equations can be written as[2]

$$A_{xx}u_x = \beta^2 u_x, \tag{1a}$$

$$A_{yy}u_y = \beta^2 u_y, \tag{1b}$$

with

$$A_{xx}u_x = \frac{\partial}{\partial x}\left[\frac{1}{n^2}\frac{\partial(n^2u_x)}{\partial x}\right] + \frac{\partial^2 u_x}{\partial y^2} + k_0^2 n^2 u_x, \tag{2a}$$

$$A_{yy}u_y = \frac{\partial^2 u_y}{\partial x^2} + \frac{\partial}{\partial y}\left[\frac{1}{n^2}\frac{\partial(n^2u_y)}{\partial y}\right] + k_0^2 n^2 u_y, \tag{2b}$$

where k_0 is the wave number in free space, $n = n(x, y)$ is the refractive index profile of the guiding medium, $\beta = k_0 n_{\text{eff}}$ is the propagation constant and n_{eff} is the effective index. u_x and u_y are the electric components in x- and y-direction, respectively. The above two equations are the scalar wave equations with polarization correction which correspond to the quasi-transverse electric (TE) and the quasi-transverse magnetic (TM) wave equations, respectively. This assumption is accurate for three classes of waveguides[1]: 1) weakly guiding waveguides with arbitrary shape and small difference in refractive indices between core and cladding or substrate; 2) arbitrary refractive index profile waveguides with an elongated or slab-like cross section; and 3) rectangular core waveguides with arbitrary core-cladding refractive index operated in the far-from cutoff region.

Figure 1 shows the finite difference mesh used in our approach for a rib waveguide. The structure is scanned with small rectangular sub-regions of size $\Delta x \times \Delta y$. Inside each sub-region the refractive index is constant, so the discontinuities of the refractive index profile occur only at the boundaries between adjacent sub-regions. In

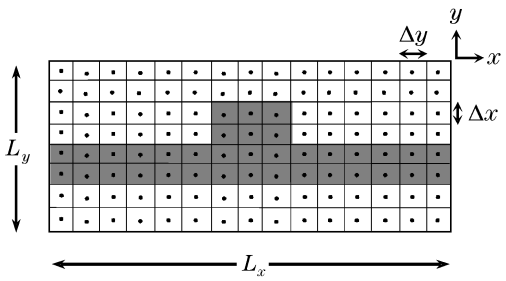

Fig. 1. Finite difference mesh for a rib waveguide.

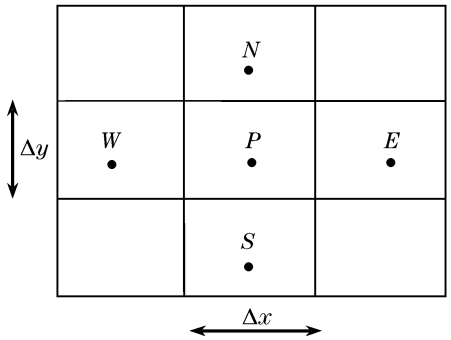

Fig. 2. Point P and neighboring points.

our finite difference scheme, the discrete points at which fields are sampled are chosen at the center of each sub-region, while some finite difference schemes select the grid points located at the vertices of each sub-region[9]. This is valid for the magnetic field which is continuous across all dielectric interfaces. For the normal component of the electric fields which is discontinuous across an abrupt dielectric interface, it will lead to vagueness. The general situation for an arbitrary grid point P with neighboring points N, S, W, and E is illustrated in Fig. 2. The refractive indices for these points are labeled as n_P, n_N, n_S, n_W, n_E, respectively.

Now we should convert the partial differential equation (1) into the corresponding finite difference equation. We first deal with the differential operator A_{xx} which operates on u_x. Because u_x is continuous across horizontal interface, the term $\frac{\partial^2 u_x}{\partial y^2}$ can be approximated with the conventional three-point difference, that is

$$\left.\frac{\partial^2 u_x}{\partial y^2}\right|^P \approx \frac{1}{(\Delta y)^2}\left(u_x^N - 2u_x^P + u_x^S\right), \tag{3}$$

where u_x^P stands for the field u_x at point P. As we know, when there is an index discontinuity between W and P or between E and P, u_x will be discontinuous, the finite difference equations must consider these discontinuities. We introduce a polynomial interpolation procedure to do this. A piecewise quadratic polynomial, defined as follows, is used to fit u_x^W, u_x^P, and u_x^E:

$$f(x) = \begin{cases} a^W + bx + cx^2 & \text{in sub}-\text{region } W \\ a^P + bx + cx^2 & \text{in sub}-\text{region } P \\ a^E + bx + cx^2 & \text{in sub}-\text{region } E \end{cases}. \tag{4}$$

The function $f(x)$ is satisfied with the conditions

$$\begin{cases} u_x^W = a^W - b\Delta x + c(\Delta x)^2 \\ u_x^P = a^P \\ u_x^E = a^E + b\Delta x + c(\Delta x)^2 \end{cases}. \tag{5}$$

Considering that the $n^2 u_x$ should be continuous at $x = \pm\frac{\Delta x}{2}$ (local coordinate system), that is

$$\begin{cases} n_W^2\left[a^W - \frac{1}{2}b\Delta x + \frac{1}{4}c(\Delta x)^2\right] \\ \quad = n_P^2\left[a^P - \frac{1}{2}b\Delta x + \frac{1}{4}c(\Delta x)^2\right] \\ n_P^2\left[a^W + \frac{1}{2}b\Delta x + \frac{1}{4}c(\Delta x)^2\right] \\ \quad = n_E^2\left[a^E + \frac{1}{2}b\Delta x + \frac{1}{4}c(\Delta x)^2\right] \end{cases}, \tag{6}$$

we have

$$\frac{\partial^2 f(x)}{\partial x^2} = \frac{1}{(\Delta x)^2}\left(\delta_W u_x^W - \delta_P u_x^P + \delta_E u_x^E\right), \tag{7}$$

with

$$\begin{cases} \delta_W = \frac{4\left(n_W^2 n_P^2 + n_W^2 n_E^2\right)}{n_P^4 + 2n_E^2 n_P^2 + 2n_W^2 n_P^2 + 3n_E^2 n_W^2} \\ \delta_P = \frac{4\left(2n_P^4 + n_E^2 n_P^2 + n_W^2 n_P^2\right)}{n_P^4 + 2n_E^2 n_P^2 + 2n_W^2 n_P^2 + 3n_E^2 n_W^2} \\ \delta_E = \frac{4\left(n_E^2 n_P^2 + n_W^2 n_E^2\right)}{n_P^4 + 2n_E^2 n_P^2 + 2n_W^2 n_P^2 + 3n_E^2 n_W^2} \end{cases}. \tag{8}$$

So the term $\frac{\partial}{\partial x}\left[\frac{1}{n^2}\frac{\partial(n^2 u_x)}{\partial x}\right]$ is approximated as

$$\left.\frac{\partial}{\partial x}\left[\frac{1}{n^2}\frac{\partial(n^2 u_x)}{\partial x}\right]\right|^P \approx \frac{1}{(\Delta x)^2}\left(\delta_W u_x^W - \delta_P u_x^P + \delta_E u_x^E\right). \tag{9}$$

Now we summarize the finite difference equation for $A_{xx}u_x$

$$A_{xx}u_x|^P = \frac{1}{(\Delta x)^2}\left(\delta_W u_x^W - \delta_P u_x^P + \delta_E u_x^E\right) + \frac{1}{(\Delta y)^2}\left(u_x^N - 2u_x^P + u_x^S\right) + k_0^2 n_P^2. \tag{10}$$

Similar procedure can also be used to derive the finite difference equations for $A_{yy}u_y$, and then Eq. (1) is converted into a standard matrix eigenvalue equation, which can be solved by using MATLAB subroutines. In order to avoid the nonphysical reflection, the absorbing boundary conditions[10] are introduced to deal with the grid points at the edge of the computational window. Moreover, Eq. (1) can be easily adopted to the non-uniform mesh grids.

The present quasi-vector finite difference method (QV-FDM) is first used to study a buried rectangular waveguide with the core of width w and height h, as shown in Fig. 3. The core refractive index $n_2 = 1.5$ at wavelength

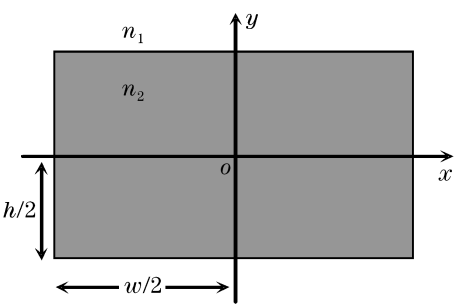

Fig. 3. Cross section of a buried rectangular waveguide.

Table 1. Normalized Propagation Constants for a Buried Rectangular Waveguide as a Function of the Cladding Refractive Index Computed by Different Methods

n_1	Scalar	Quasi-TE Mode		Quasi-TM Mode	
	FDM[10]	QV-NLIM[11]	QV-FDM	QV-NLIM[11]	QV-FDM
1.45	0.5125	0.5090	0.5091	0.4996	0.4997
1.40	0.5125	0.5052	0.5053	0.4860	0.4861
1.20	0.5125	0.4897	0.4898	0.4258	0.4259

$\lambda = 1.15$ μm with $w/h = 2$. The normalized frequency, V, is defined as

$$V = \frac{h}{\lambda}\sqrt{n_2^2 - n_1^2}. \tag{11}$$

The normalized propagation constant, B, is defined as

$$B = \frac{n_{\text{eff}}^2 - n_2^2}{n_2^2 - n_1^2}. \tag{12}$$

Table 1 presents the normalized propagation constants B of the quasi-vector fundamental mode as a function of the cladding index n_1 in the buried rectangular waveguide with $V = 1.0$. The grid size in the core and its neighboring cladding is $\Delta x = \Delta y = 0.05$ μm, and the grid size in the other claddings is $\Delta x = \Delta y = 0.1$ μm. In order to test the accuracy of the present method, the results obtained by scalar FDM[11] and quasi-vector nonlinear iterative method (QV-NLIM)[12] which has been proved highly accurate are also summarized in the table. It can be seen that the results obtained by our method and the QV-NLIM agree well with each other. Moreover, the difference between the scalar and quasi-vector solutions gradually increases with the increment of the refractive-index contrast between the core and the cladding regions. The scalar wave equation is valid only for the weakly guiding waveguides. Figure 4 plots the field distributions of the quasi-vector fundamental modes for the buried rectangular waveguide with $w = 2.0$ μm, $h = 1.0$ μm, $n_1 = 1.2$, $n_2 = 1.5$, and $\lambda = 1.15$ μm. The discontinuities across the core and the cladding interface for the quasi-TE mode along x-direction and the quasi-TM mode along y-direction are visible.

Next, we analyze a typical rib waveguide whose cross section is shown in Fig. 5. Here, the rib width $w = 3.0$ μm, the rib height $h = 1.0$ μm, the superstratum index $n_1 = 1.0$, the core index $n_2 = 3.44$, and the substrate index $n_3 = 3.36$ with the wavelength $\lambda = 1.15$ μm. In the superstrate (air), coarse grid size, $\Delta x = \Delta y = 0.05$ μm, is used, while in the core and the substrate, fine grid size, $\Delta x = \Delta y = 0.02$ μm, is used. The normalized propagation constants B of the quasi-vector TE and TM modes as a function of the slab waveguide height t are presented in Table 2. The results obtained by full-vector beam propagation method (FV-BPM)[13] are also included in this table. It is seen that the difference between our results

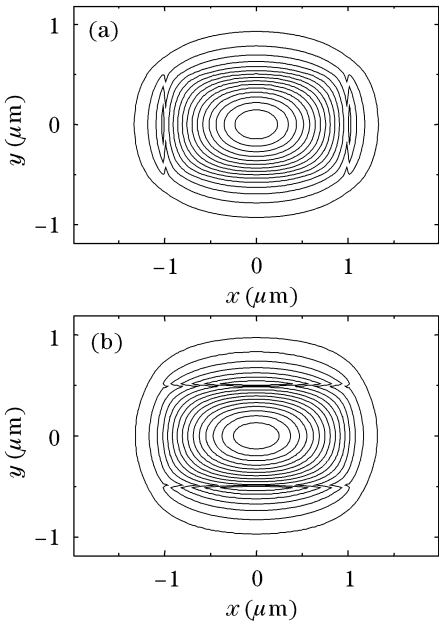

Fig. 4. Field distributions of quasi-TE (a) and quasi-TM (b) fundamental modes for a buried rectangular waveguide.

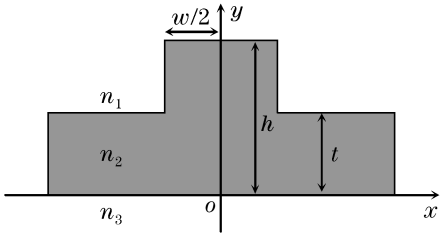

Fig. 5. Cross section of a rib waveguide.

Table 2. Normalized Propagation Constants for a Rib Waveguide as a Function of the Slab Waveguide Height Computed by Different Methods

t	Scalar	Quasi-TE Mode		Quasi-TM Mode	
(μm)	FDM[10]	FV-BPM[12]	QV-FDM	FV-BPM[12]	QV-FDM
0.1	0.3094	0.3039	0.3020	0.2690	0.2668
0.3	0.3179	0.3144	0.3110	0.2776	0.2743
0.5	0.3330	0.3303	0.3279	0.2915	0.2895
0.7	0.3563	0.3533	0.3520	0.3127	0.3111
0.9	0.3914	0.3879	0.3871	0.3451	0.3437

and the solutions from FV-BPM is relatively small for the rib waveguide with large slab waveguide height in which the fundamental modes are far-from cutoff. In this case, unless the polarization dependence of the guided-modes is of interest, the quasi-vector results should be sufficient. However, for the rib waveguide with small slab waveguide height, full-vector mode solver is needed. Figure 6 illustrates the field patterns of the quasi-TE and quasi-TM fundamental modes with $t = 0.3$ μm. Here again the respected discontinuities are observed.

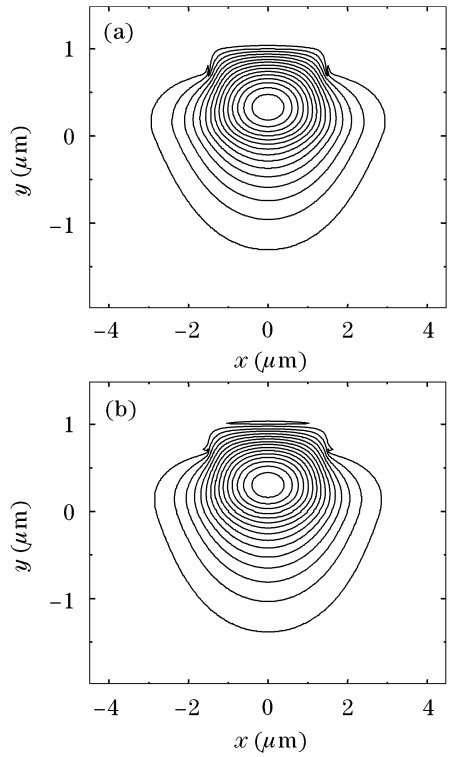

Fig. 6. Field distributions of quasi-TE (a) and quasi-TM (b) fundamental modes for a rib waveguide.

In conclusion, a finite difference scheme based on the polynomial interpolation in solving the quasi-vector wave equations for optical waveguides with step-index profiles is described. The discontinuities of the normal components of the electric field across abrupt dielectric interfaces are successfully observed. Moreover, the quasi-vector results include the polarization effects, but the order of the resulted matrix is the same as that for scalar wave equation. Therefore, the computational time is moderate in comparison with the full-vector results. The accuracy of the present approach is comparable to the methods published earlier for a buried rectangular waveguide and a typical rib waveguide.

J. Xiao's e-mail address is jbxiao@seu.edu.cn.

References

1. C. Vassallo, Opt. Quantum Electron. **29,** 95 (1997).
2. R. Scarmozzino, A. Gopinath, R. Pregla, and S. Helfert, IEEE J. Sel. Top. Quantum Electron. **6,** 150 (2000).
3. S. Guo, F. Wu, S. Albin, H. Tai, and R. Rogowski, Opt. Express **12,** 3341 (2004).
4. K. Saitoh, M. Koshiba, and Y. Tsuji, J. Lightwave Technol. **17,** 255 (1999).
5. J. Xiao, X. Sun, M. Zhang, and D. Ding, Acta Opt. Sin. (in Chinese) **22,** 201 (2002).
6. J. Xiao, X. Sun, and M. Zhang, J. Opt. Soc. Am. B **21,** 798 (2004).
7. E. Schweig and W. B. Bridges, IEEE Trans. Microwave Theory and Techniques **32,** 531 (1984).
8. G. R. Hadley and R. E. Smith, J. Lightwave Technol. **13,** 465 (1995).
9. P. Lüsse, K. Ramm, H.-G. Unger, and J. Schüle, Opt. Quantum Electron. **29,** 115 (1997).
10. D. Jiménez and F. Pérez-Murano, J. Opt. Soc. Am. A **18,** 2015 (2001).
11. M. S. Stern, IEE Proceedings J **138,** 185 (1991).
12. S. Sujecki, T. M. Benson, P. Sewell, and P. C. Kendall, J. Lightwave Technol. **16,** 1329 (1998).
13. W. P. Huang and C. L. Xu, IEEE J. Quantum Electron. **29,** 2639 (1993).